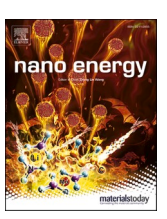
ELSEVIER

Contents lists available at ScienceDirect

## Nano Energy

journal homepage: www.elsevier.com/locate/nanoen





# High-throughput screening of protective layers to stabilize the electrolyte-anode interface in solid-state Li-metal batteries

Simo Li, Zhefeng Chen, Wentao Zhang, Shunning Li<sup>\*</sup>, Feng Pan<sup>\*</sup>

School of Advanced Materials, Peking University, Shenzhen Graduate School, Shenzhen 518055, PR China

ARTICLE INFO

Keywords:
Li-metal batteries
Solid-state electrolytes
Protective layer
Electrolyte-anode interface
High-throughput computational screening

#### ABSTRACT

Solid-state Li-metal batteries have attracted growing interest over the years as a promising candidate for next-generation energy storage. Yet, the Li metal not only spontaneously reacts with most solid-state electrolytes (SSEs), but also triggers Li dendrite growth in the SSEs at a lower current density than traditional liquid electrolytes. Buffering the electrolyte-anode interface with a protective layer could be a viable solution to this problem. Herein, we search for candidate protective-layer materials from 2316 experimentally known Licontaining compounds using high-throughput first principles calculations. Tiered screening of both stability and electronic structure allows the identification of 5, 28 and 7 materials as suitable for protecting  $\text{Li}_7\text{La}_3\text{Zr}_2\text{O}_{12}$ ,  $\text{Li}_3\text{PS}_4$  and  $\text{LiTi}_2(\text{PO}_4)_3$ , respectively. We demonstrate that electron transfer from Li metal to SSE is successfully blocked by the protective layer to restrain the dendrite growth. This work enables a significant reduction of search space for materials discoveries in protective layer for solid-state Li-metal batteries.

#### 1. Introduction

Rechargeable solid-state Li-metal batteries have long been proposed as the next-generation energy storage devices due to their high theoretical specific capacity and the non-flammability characteristic [1–6]. The most critical component in a solid-state Li-metal battery is the solid-state electrolyte (SSE), which requires both high ionic conductivity and good electrochemical stability [7,8]. Over the past years, a number of promising SSEs have been discovered [9-15], among which  $\text{Li}_7\text{La}_3\text{Zr}_2\text{O}_{12}$  (LLZO) [16],  $\text{Li}_3\text{PS}_4$  (LPS) [17] and  $\text{Li}_{1+r}\text{Al}_r\text{Ti}_{2-r}(\text{PO}_4)_3$ (LATP) [18] are the most extensively studied and exploited. However, even though many efforts have been devoted to this area, the solid-state Li-metal batteries are still far from practical application [19–21]. One of the most pernicious problems is the propensity of lithium dendrite propagation inside these SSEs at low critical current density, even beneath that in nonaqueous liquid electrolytes [22-25]. The SSEs may also react with Li metal, forming unstable solid electrolyte interphase layer that impairs the battery performance [26]. Therefore, it is a crucial challenge to develop strategies for the mitigation of unwanted interaction between SSEs and Li-metal anode.

Introducing a protective layer could be a viable means to manipulate the interface between SSEs and Li metal (Fig. 1a), and some inspiring progress has been made in this direction recently [27–30]. The major

benefit of protective layers is in blocking the electron transfer from Li metal to the SSEs during charging. In the ideal cases, the conduction bands of SSEs should be high enough to guarantee that no excess electron is trapped in their bulk or interfaces during Li deposition (Fig. 1b). However, for LLZO, LPS and LAPT, their conduction band minimum (CBM) at the surface is below the energy level of Li plating (i.e., the Li<sup>+</sup>/Li<sup>0</sup> potential), as reported in previous studies [31,32], and hence their electrical contact with Li metal will inevitably trigger electron transfer (Fig. 1c). The polarons induced by this electron transfer will lead to both parasitic reactions and disastrous formation of Li dendrites penetrating the SSEs along the grain boundaries. In comparison, a protective layer featuring a high CBM and a wide band gap can pose a direct barrier to prevent such electron transfer (Fig. 1d), thus conferring improved electrochemical performance to the solid-state Li-metal batteries. The advantages of stabilized electrolyte-anode interface have been well documented in the studies using protective layers such as LiF, ZnO, h-BN, et al. [28,33-39]. Despite the limited Li ion diffusivity in the protective layers and across the interfaces, striking improvements in battery performance were unequivocally demonstrated in these works. Nevertheless, a rationale screening of candidate materials from the family of inorganic compounds is still not available so far. While experimental exploration in this endeavor would have proved labor intensive, one promising alternative may lie in the high-throughput

E-mail addresses: lisn@pku.edu.cn (S. Li), panfeng@pkusz.edu.cn (F. Pan).

<sup>\*</sup> Corresponding authors.

computational approaches, given their past success in predicting potential cathode coatings for Li-ion batteries [40-42].

Herein, we perform high-throughput density functional theory (DFT) calculations to screen all Li-containing materials in Inorganic Crystal Structure Database (ICSD) [43] for those with wide electrochemical stability window, low chemical reactivity, large band gap and especially, with CBM above the  ${\rm Li}^+/{\rm Li}^0$  potential. Only Li-containing materials are considered because intrinsic Li content is beneficial for facile Li diffusion across the thin protective layer. LLZO, LPS and  ${\rm LiTi}_2({\rm PO}_4)_3$  (LTP) are chosen as the representative SSEs, for each of which we identify a set of appropriate protective-layer materials through tiered screening. We find that from a total of 2316 candidate materials, only 5, 28 and 7 can be adopted for protecting LLZO, LPS and LTP, respectively. Halides and polyanionic oxides constitute the majority of materials for use as protective layers, which can be tested in future experimental investigations.

#### 2. Computational methods

All the calculations were performed within a plane-wave basis set and the projector augmented wave (PAW) method, as implemented in the Vienna ab initio simulation package (VASP) [44,45]. Perdew-Burke-Ernzerhof (PBE) [46] exchange and correlation

functional of generalized gradient approximation (GGA) [47] was employed. The energy cut-off of the plane waves was set to 520 eV, and the Monkhorst-Pack k-point grids [48] were set to at least 1000/(the number of atoms per cell) for all calculations. Phase diagram of each compound was obtained from the Materials Project database [49] within the same computational scheme. Activation energy barriers for Li diffusion were estimated via softBV method [50].

The phase stability was estimated by calculating the energy convex hull and phase diagram at 0 K, taking into consideration all known crystalline materials using the pymatgen package [51]. Energy above convex hull ( $E_{\rm hull}$ ) is defined as the energy per atom of the corresponding compound above the stable phase at the same composition in the phase diagram. If a compound has positive  $E_{\rm hull}$ , it tends to decompose into another phase upon disturbance. Considering the kinetic constraints during phase transition, a threshold on the scale of meV/atom was generally set for  $E_{\rm hull}$  to filter out the highly unstable compounds in the screening process [41].

The electrochemical stability window was estimated via lithium grand potential phase diagram. We considered the grand potential  $\Phi$  of a compound using the following equation:

$$\Phi[c, \mu_{Li}] = E[c] - n_{Li}[c]\mu_{Li}$$
(1)

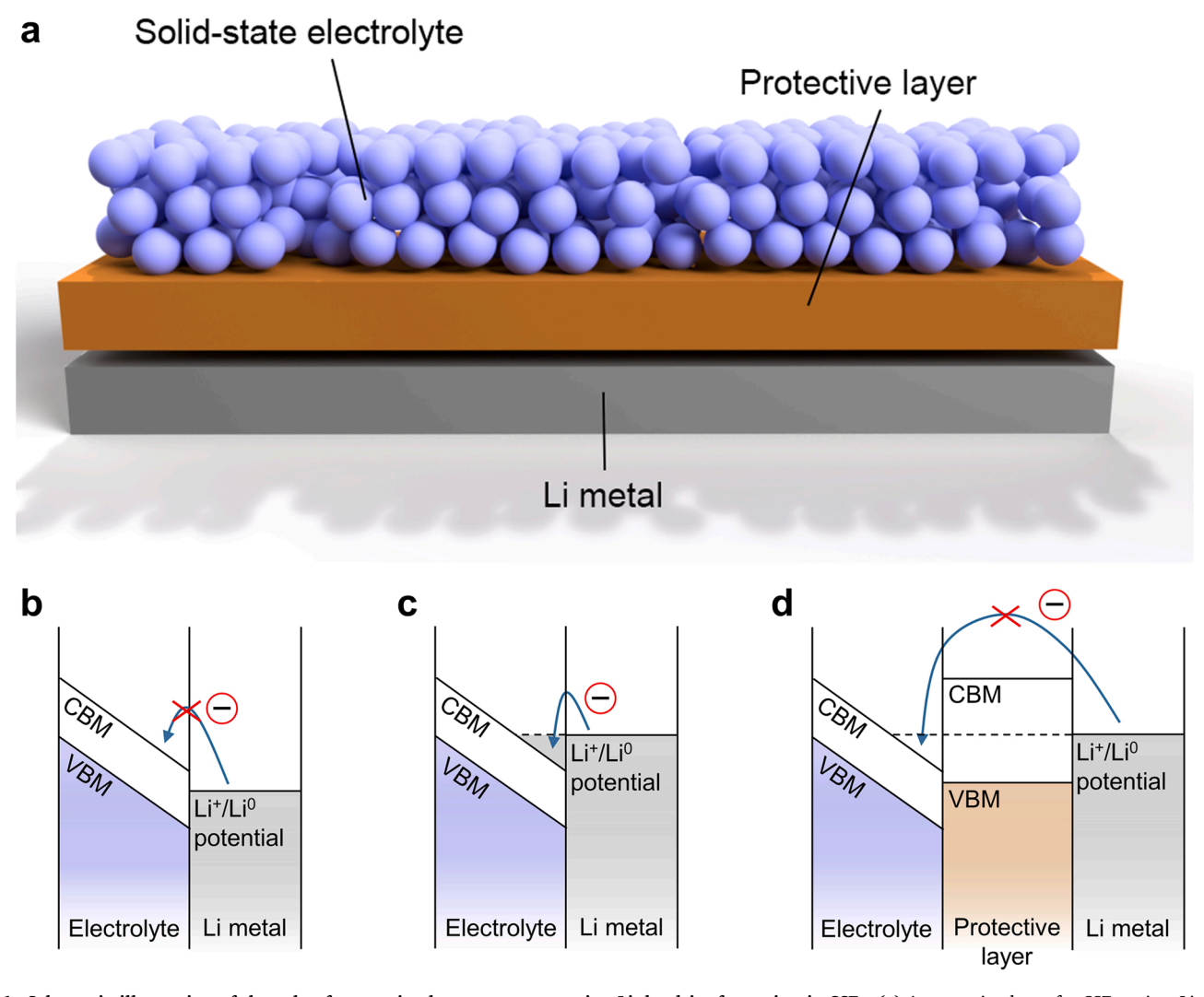


Fig. 1. Schematic illustration of the role of protective layers on suppressing Li dendrite formation in SSEs. (a) A protective layer for SSE against Li-metal anode. (b) Band structure of the ideal cases where the CBM of SSE is above the  ${\rm Li^+/Li^0}$  potential. (c) Band structure of the actual situation where the CBM of SSE is beneath the  ${\rm Li^+/Li^0}$  potential, leading to electron transfer and dendrite formation in SSE during Li deposition. (d) Band structure of the cases where a protective layer is introduced to block the electron transfer.

Nano Energy 102 (2022) 107640

where c is the composition of the material, E[c] is the enthalpy,  $n_{\rm Li}[c]$  is the Li concentration, and  $\mu_{\rm Li}$  is the lithium chemical potential. The grand potential range within which the compound is stable would correspond to its electrochemical stability window [52,53]:

$$V_{\rm red} = \frac{\mu_{\rm Li}^0 - \mu_{\rm red}}{e} \tag{2}$$

$$V_{\text{oxi}} = \frac{\mu_{\text{Li}}^0 - \mu_{\text{oxi}}}{e} \tag{3}$$

where  $V_{\rm red}$  and  $V_{\rm oxi}$  are the reduction potential and the oxidation potential of the electrochemical stability window;  $\mu_{\rm Li}^0$ ,  $\mu_{\rm red}$  and  $\mu_{\rm oxi}$  are the Li chemical potentials of Li metal, the reduction limit and the oxidation limit in phase diagram, respectively; e is the elementary charge.

The chemical stability was estimated according to the chemical reaction energy between two substances following the methodology proposed by Richards et al. [54]. For two reactants  ${\bf a}$  and  ${\bf b}$ ,  $\Delta E_{{\bf a},{\bf b}}$  was determined according to the mixing ratio  ${\bf x}$  that yields the largest reaction driving force:

$$\Delta E_{\mathbf{a},\mathbf{b}} = \min_{x \in [0,1]} \left\{ E_{\text{pd}} [xc_{\mathbf{a}} + (1-x)c_{\mathbf{b}}] - xE[c_{\mathbf{a}}] - (1-x)E[c_{\mathbf{b}}] \right\}$$
(4)

where  $c_a$  and  $c_b$  are the compositions of reactants a and b normalized by the numbers of atoms, and  $E_{pd}[c]$  is the ground-state energy of equilibrium phase at the composition c [54].

Tetragonal Li $_7$ La $_3$ Zr $_2$ O $_{12}$  (t-LLZO) was selected to represent LLZO, since previous study reported that this phase predominates at the interface with Li metal [55]. For LPS,  $\beta$ -Li $_3$ PS $_4$  was employed as commonly used. For LTP, LiTi $_2$ (PO $_4$ ) $_3$  with a space group of R-3c was considered in this study.

#### 3. Results and discussion

In ICSD, there are 2316 Li-containing materials that do not exhibit fractional occupancy at lattice sites, which constitutes the basis for high-throughput computational screening. As a prerequisite for application in electrochemical energy storage, the protective layer should be thermodynamically stable against decomposition into other phases. Thermodynamic stability of a compound can be evaluated by its ground-state convex hull at 0 K, and the energy above this hull could be regarded as the driving force for phase transition into the ground-state configuration at the corresponding composition. Here we follow the work of Ceder et al. [41] who set a criterion of 5 meV/atom for energy above hull to filter out the unstable compounds. The pool of candidate materials for protective layer shrinks by around 40% after this screening tier (Fig. S1).

After the phase stability evaluation, we examine the electrochemical stability of the candidate compounds. The electrochemical stability window corresponds to the voltage range in which the compound is stable without electrochemical reactions. The oxidation and reduction limits are defined as the voltage thresholds at which the compound tends

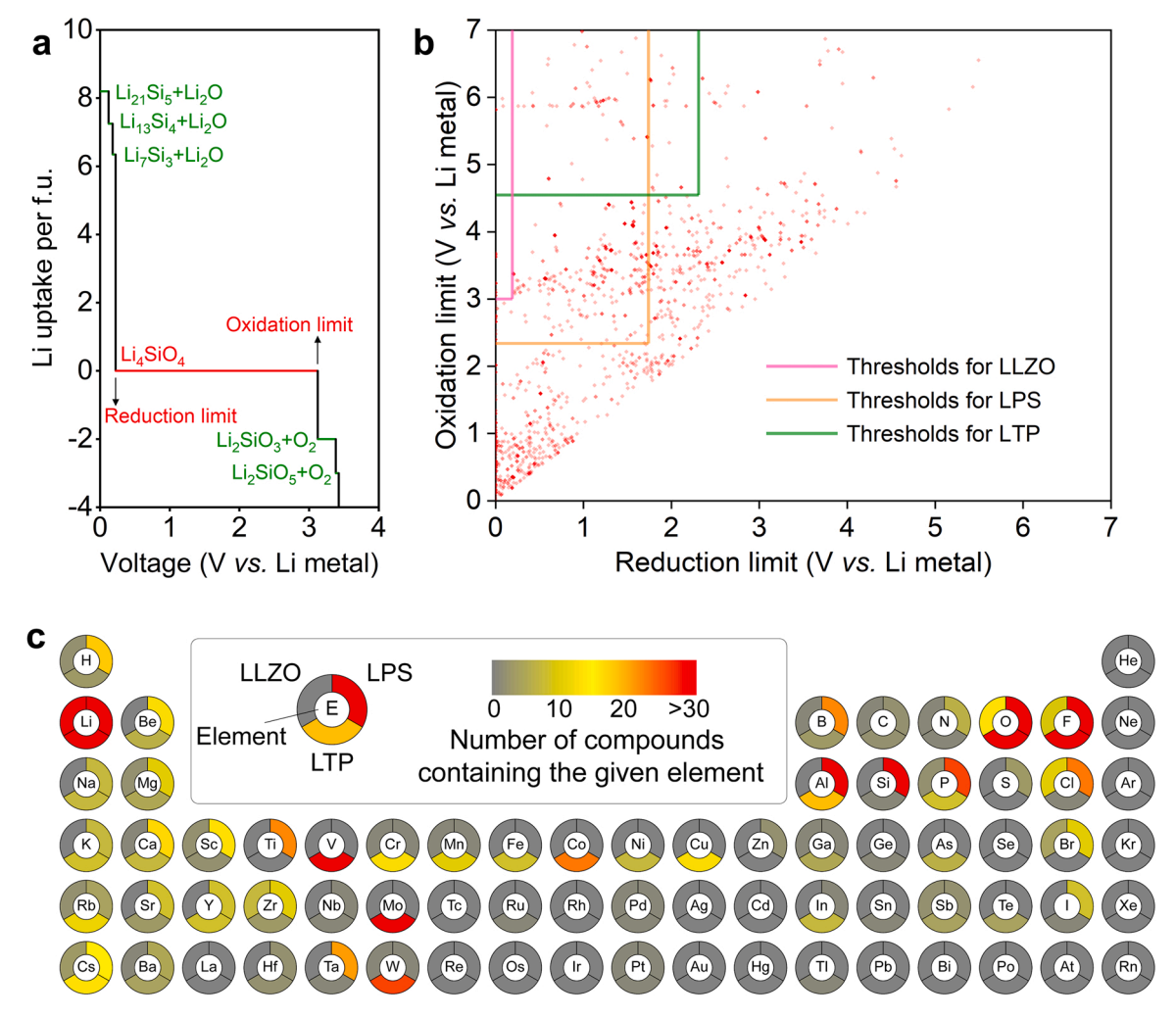


Fig. 2. Electrochemical stability screening results. (a) The voltage profile during electrochemical oxidation and reduction of Li<sub>4</sub>SiO<sub>4</sub>. (b) Electrochemical stability window of all the candidate materials for use as protective layer. Each material is represented by a dot. (c) Number of candidate compounds containing a given element. The results of potential protective layers for LLZO, LPS and LTP are provided separately.

S. Li et al. Nano Energy 102 (2022) 107640

to undergo Li extraction and insertion, respectively. For example, the oxidation of Li<sub>4</sub>SiO<sub>4</sub> begins at 3.12 V vs. Li metal, forming Li<sub>2</sub>SiO<sub>3</sub> and O2, while the reduction of Li<sub>4</sub>SiO<sub>4</sub> begins at 0.22 V, leading to the emergence of Li<sub>7</sub>Si<sub>3</sub> and Li<sub>2</sub>O (Fig. 2a). Similarly, we calculate the oxidation and reduction limits of all the potential Li-containing compounds for use as protective layer (Fig. 2b). The criteria for electrochemical stability screening can be defined according to the electrochemical stability windows of LLZO, LPS and LTP, respectively (Table S1). Since the formation of new phases is likely to be inhibited by kinetic factors, an overpotential is generally required to initiate the oxidation/reduction reaction [56]. In this regard, we set a criterion that the electrochemical stability window of a protective layer should cover 90% of the operating voltage range for the selected SSE (LLZO/LPS/LTP). The thresholds are highlighted in Fig. 2b. After this screening tier, there remain 34, 478 and 187 candidate protective-layer materials for LLZO, LPS and LTP, respectively. In Fig. 2c, we summarize the number of candidate materials containing a specific chemical element (denoted as "E"). It is apparent that main group elements are rather popular, such as O, F, Al and Si, while a relatively low chemical diversity is witnessed for transition metal elements, with only few of them (Ti, V, Mo and W) being prevalent in the candidate materials.

Then we evaluate the chemical stability against the targeted SSE (LLZO/LPS/LTP). Chemical stability can be quantified by the most negative reaction energy ( $\Delta E$ ) of all possible chemical mixing reactions between the protective layer and the SSE. A threshold of  $|\Delta E| \leq 100$  meV/atom could guarantee low reactivity and was therefore set as the criterion. After this screening tier, a large number of fluorides are discarded due to their strong interaction with the electrolyte materials. We would like to note that Li<sub>2</sub>CO<sub>3</sub> is easily formed on LLZO surface because of the exposure to humid air, which leads to large interfacial impedance [57,58]. If LLZO is well sealed during its synthesis and application, the Li<sub>2</sub>CO<sub>3</sub> formation could be effectively inhibited. Therefore, we believe that the introduction of a protective layer with high chemical stability could simultaneously address the problem of Li<sub>2</sub>CO<sub>3</sub> formation, which rescinds the concerns about reaction between SSE and external substances.

Besides these stability metrics, the most important property of a protective layer at the electrolyte-anode interface is a suitable electronic structure that can prevent electron transfer from the Li-metal anode to the SSE. To this end, the protective layer should be electronically insulating with conduction bands high enough to block electron injection from the Li metal. Therefore, we design two search principles: (1) The bandgap should be at least 2 eV and (2) the CBM should be above the Li<sup>+</sup>/Li<sup>0</sup> potential. After this round of screening, the candidate compounds are narrowed down to 5, 28 and 7 for the protection of LLZO, LPS and LTP, respectively. Fig. 3 provides a thorough list of the candidate compounds and displays their band edges in comparison with the Li<sup>+</sup>/Li<sup>0</sup> potential (-1.39 eV vs. vacuum level [10]). We note that halides and polyanionic oxides account for 80% of the candidate materials, and some of them have already made their appearance in the literature as effective buffer layers, such as LiF [27,59], LiI [60], Li<sub>3</sub>BO<sub>3</sub> [61] and Li<sub>2</sub>SiO<sub>3</sub> [62]. In principle, the band alignment of these protective-layer materials can serve to suppress the Li dendrite formation inside SSEs. The reason for halides and polyanionic oxides occupying the majority could be the high ionicity and low covalency between Li and anions in these compounds. The ionic character gives rise to high energy level of the empty Li-s states at the bottom of conduction bands, which could raise opportunities to surpass the Li<sup>+</sup>/Li<sup>0</sup> potential.

To provide a more comprehensive scenario of how the protective layer interacts with both SSEs and Li metal to hinder electron transfer, we further investigate these interfaces via DFT calculations. We first study the equilibrium shapes of LLZO, LPS and LTP via Wulff construction, taking into consideration their low Miller-index stoichiometric surfaces. The surface models of these SSEs are depicted in Fig. S2-S4, and the calculation results of surface energy are listed in Table S2-4. We note that the (101) surface of LLZO, the (210) surface of LPS and the

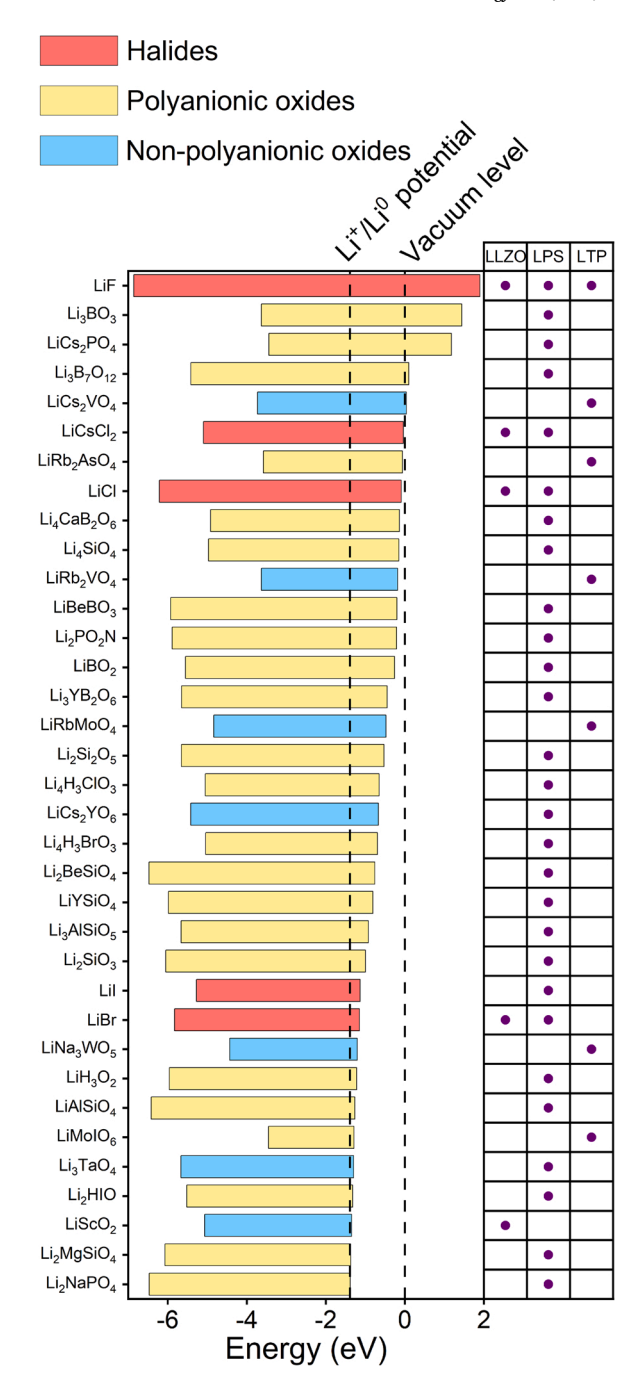


Fig. 3. Valence band maximum (the left end of the bar) and conduction band minimum (the right end of the bar) of the compounds that pass the high-throughput screening in this work. Energy is referenced to the vacuum level. The purple dots on the right of the diagram indicate which SSE the protective layer is suitable for.

(012) surface of LTP exhibit the highest ratios in surface area (details provided in Supporting Information). Accordingly, they are chosen as the representative surfaces for these SSEs. Example models of LLZO (101)|LiCl(001), LPS(210)|LiBO<sub>2</sub>(001) and LTP(012)|LiF(001) interfaces are constructed, as shown in Fig. 4a-c. We have examined their interfacial energies, which turn out to be exothermic (Table S5), suggesting the formation of intimate interfaces. We calculate the charge density difference corresponding to the interaction at the interface, and find that no charge transfer across the interface is observed, although a certain degree of polarization is induced in the protective-layer materials. The electronic density of states (DOS) indicates that all the

S. Li et al. Nano Energy 102 (2022) 107640

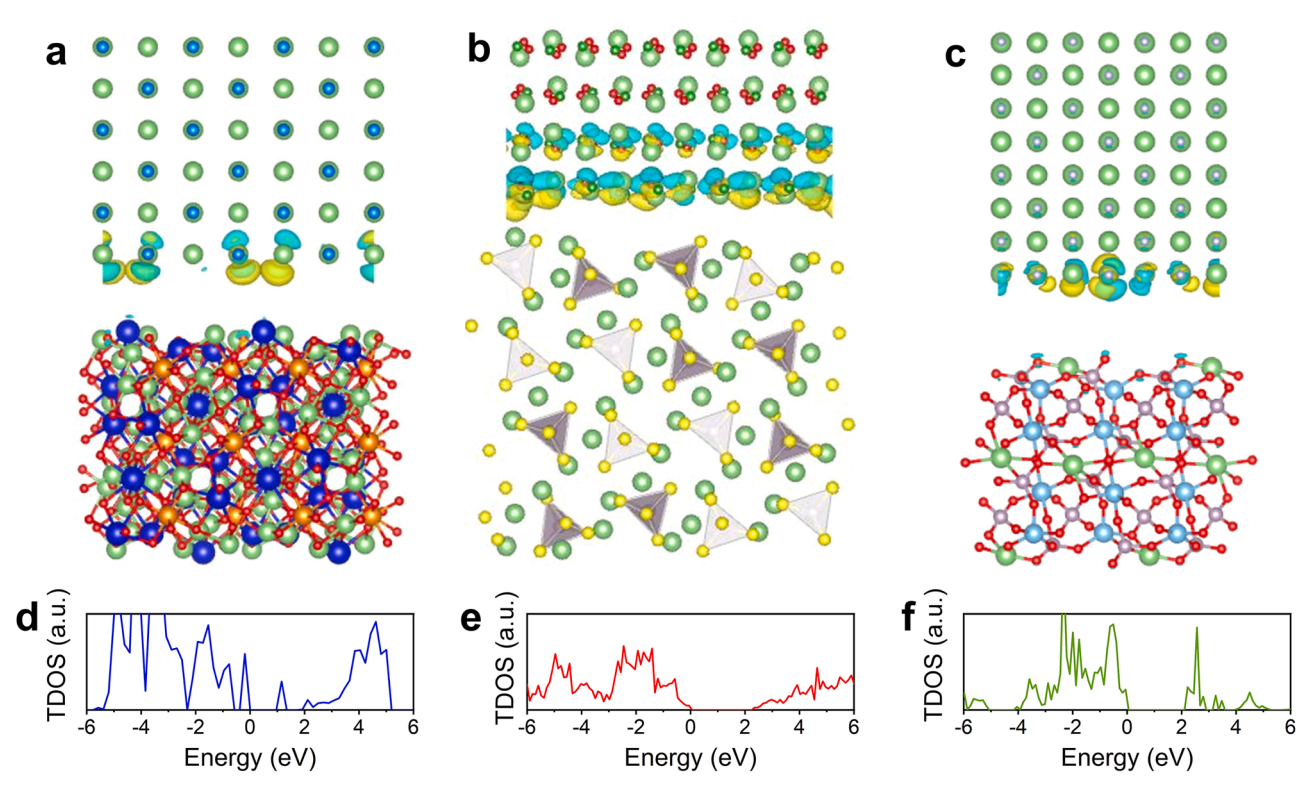


Fig. 4. Electronic structures of the LLZO(101)|LiCl(001), LPS(210)|LiBO<sub>2</sub>(001) and LTP(012)|LiF(001) interfaces. The charge density difference of (a) LLZO (101)|LiCl(001), (b) LPS(210)|LiBO<sub>2</sub>(001) and (c) LTP(012)|LiF(001) interfaces. The yellow and blue isosurfaces indicate charge accumulation and depletion regions after the formation of interface, respectively. The total density of states (TDOS) of (d) LLZO(101)|LiCl(001), (e) LPS(210)|LiBO<sub>2</sub>(001) and (f) LTP(012)|LiF(001) interfaces. Energy is referenced to the Fermi level.

interfaces remain insulating (Fig. 4d-f), which is consistent with the charge density difference results. These calculations suggest that the interfaces between protective layers and SSEs are stable and robust without formation of metallic states, and therefore the interfacial interactions could hardly affect the electron-blocking ability of the protective layer. It is also worth mentioning that additional interfacial impedance would likely be introduced into the battery after the incorporation of a protective layer, especially when the Li ion conductivity is low in this material (Table S6). Nevertheless, the thin-film nature of the protective layer means that the diffusion distance of Li ions is relatively short, and hence the overall kinetics may only be affected to a small degree. Previous experimental results of LiF and LiI [27,59,60] have justified exploiting materials with low Li ion conductivity as potential protective layers between SSEs and Li metal, demonstrating the more determinant role of electronic structure than Li diffusivity in Li dendrite growth.

Before inspecting the interface between protective layer and Li metal, we consider the electronic structures of LLZO(101)|Li(110), LPS (210)|Li(110) and LTP(012)|Li(110) interfaces. To simulate the electron transfer during Li deposition, an excess electron is introduced to each model, from which we can calculate the differential charge density between the configurations with and without an additional electron (Fig. S6). According to the differential charge density, we find that the excess electron prefers to distribute near the SSE surfaces rather than in Li metal, which is consistent with our expectation of electron transfer from Li-metal anode to the grain boundaries of SSEs during charging. Likewise, we construct the LiCl(001)|Li(110) interface and present the differential charge density in Fig. 5a. A charge accumulation region appears at the Li metal surface, indicating the localization of excess electron in Li metal, which simultaneously triggers the intensive polarization in LiCl. To further substantiate this evidence, we turn to the charge neutral model and calculate the partial charge density within an energy range of 0 ~ 1 eV vs. Fermi level (Fig. 5b). Notably, the

electronic states are mainly localized at the outermost Li layer, in good agreement with the differential charge density result. The CBM of LiCl is well above the Fermi level and no gap states emerge in the LiCl region, as illustrated in the partial DOS plots in Fig. 5c. It can be drawn from these results that electrons could not be injected from the Li metal to the interior of the protective layer during Li plating, thus eliminating the possibility of excess electron accumulation at the grain boundaries of SSEs and preventing the Li dendrite formation therein.

#### 4. Conclusions

In summary, through systematic analysis of experimentally known compounds extracted from ICSD, we establish a dedicated portfolio of protective-layer materials for stabilizing the electrolyte-anode interface in solid-state Li-metal batteries. After tiered screening of thermodynamic stability, electrochemical stability, chemical stability and electronic band structure, we discover 5, 28 and 7 Li-containing materials that are highly stable and capable of blocking electron transfer from Li metal to LLZO, LPS and LTP, respectively, and many of them have not been reported in the past. In particular, the electronic insulating nature of these protective layers could remain intact at the interfaces with SSEs and with Li-metal anode. This work drastically reduces the search space of compounds for use as protective layer to suppress Li dendrite propagation in SSEs, and the recommended materials will hopefully accelerate progress in the design of solid-state Li-metal batteries.

#### CRediT authorship contribution statement

**Simo Li**: Formal analysis, Investigation, Data curation, Writing - original draft. **Zhefeng Chen**: Formal analysis. **Wentao Zhang**: Formal analysis. **Shunning Li**: Conceptualization, Formal analysis, Writing - review & editing, Project administration, Funding acquisition. **Feng Pan**: Resources, Writing - review & editing, Supervision, Project

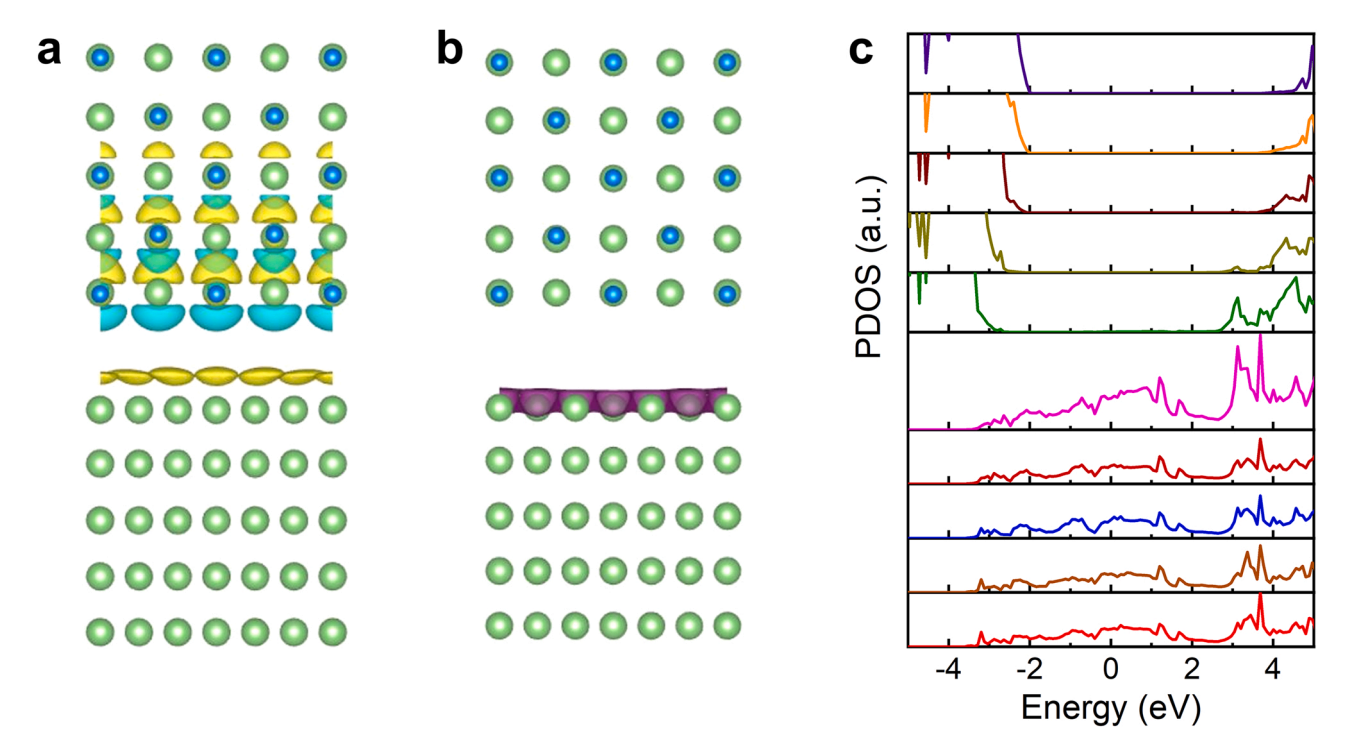


Fig. 5. Electronic structure of the LiCl(001) Li(110) interface. (a) The differential charge density between configurations with and without an excess electron in the interface model. (b) The partial charge density within an energy range of  $0 \sim 1$  eV vs. Fermi level. (c) Partial density of states (PDOS) by atomic layers. Energy is referenced to the Fermi level.

administration, Funding acquisition.

#### **Declaration of Competing Interest**

The authors declare that they have no known competing financial interests or personal relationships that could have appeared to influence the work reported in this paper.

## Data availability

Data will be made available on request.

## Acknowledgements

This work was financially supported by Soft Science Research Project of Guangdong Province (No. 2017B030301013), the National Natural Science Foundation of China (22109003), Young S&T Talent Training Program of Guangdong Provincial Association for S&T (SKXRC202211) and the Major Science and Technology Infrastructure Project of Material Genome Big-science Facilities Platform supported by Municipal Development and Reform Commission of Shenzhen.

#### Appendix A. Supporting information

Supplementary data associated with this article can be found in the online version at doi:10.1016/j.nanoen.2022.107640.

## References

- [1] X.B. Cheng, R. Zhang, C.Z. Zhao, Q. Zhang, Toward safe lithium metal anode in rechargeable batteries: a review, Chem. Rev. 117 (2017) 10403–10473.
- [2] J.B. Goodenough, Y. Kim, Challenges for rechargeable Li batteries, Chem. Mater. 22 (2009) 587–603.
- [3] M. Armand, J.-M. Tarascon, Building better batteries, Nature 451 (2008) 652-657.
- [4] W. Xu, J. Wang, F. Ding, X. Chen, E. Nasybulin, Y. Zhang, J.-G. Zhang, Lithium metal anodes for rechargeable batteries, Energy Environ. Sci. 7 (2014) 513–537.

- [5] E. Quartarone, P. Mustarelli, Electrolytes for solid-state lithium rechargeable batteries: recent advances and perspectives, Chem. Soc. Rev. 40 (2011) 2525–2540.
- [6] J.-M. Tarascon, M. Armand, Prelithiation activates Li(Ni0.5Mn0.3Co0.2)O2 for high capacity and excellent cycling stability, Nature 414 (2001) 359–367.
- [7] L. Fan, S. Wei, S. Li, Q. Li, Y. Lu, Recent progress of the solid-state electrolytes for high-energy metal-based batteries, Adv. Energy Mater. 8 (2018), 1702657.
- [8] Y. Lu, X. Chen, C.-Z. Zhao, Q. Zhang, Chin. J. Struct. Chem. 39 (2020) 8–10.
- [9] Q. Zhao, S. Stalin, C.-Z. Zhao, L.A. Archer, Adolescent haze-related knowledge level study: a cross-sectional survey with sensitivity analysis, Nat. Rev. Mater. 5 (2020) 229–252
- [10] A. Manthiram, X. Yu, S. Wang, Lithium battery chemistries enabled by solid-state electrolytes, Nat. Rev. Mater. 2 (2017) 16103.
- [11] Y.-S. Hu, Batteries: getting solid, Nat. Energy 1 (2016) 16042.
- [12] C. Wang, K. Fu, S.P. Kammampata, D.W. McOwen, A.J. Samson, L. Zhang, G. T. Hitz, A.M. Nolan, E.D. Wachsman, Y. Mo, V. Thangadurai, L. Hu, Garnet-type solid-state electrolytes: materials, interfaces, and batteries, Chem. Rev. 120 (2020) 4257–4300.
- [13] Q. Zhang, D. Cao, Y. Ma, A. Natan, P. Aurora, H. Zhu, Sulfide-based solid-state electrolytes: synthesis, stability, and potential for all-solid-state batteries, Adv. Mater. 31 (2019), e1901131.
- [14] E. Umeshbabu, B. Zheng, Y. Yang, Recent progress in all-solid-state lithium—sulfur batteries using high Li-ion conductive solid electrolytes, Electrochem. Energy Rev. 2 (2019) 199–230.
- [15] X.-L. Xue, X.-X. Zhang, J.-H. Lin, S.-J. Chen, Y.-Q. Chen, Y.-C. Liu, Y.-N. Zhang, Chin. J. Struct. Chem. 39 (2020) 1941–1948.
- [16] R. Murugan, V. Thangadurai, W. Weppner, Fast lithium ion conduction in garnettype Li(7)La(3)Zr(2)O(12), Angew. Chem. Int. Ed. 46 (2007) 7778–7781.
- [17] Z. Liu, W. Fu, E.A. Payzant, X. Yu, Z. Wu, N.J. Dudney, J. Kiggans, K. Hong, A. J. Rondinone, C. Liang, Anomalous high ionic conductivity of nanoporous β-Li3PS4, J. Am. Chem. Soc. 135 (2013) 975–978.
- [18] J. Fu, Estimating the age of the common ancestor of a sample of DNA sequences, Solid State Ion. 96 (1997) 195–200.
- [19] K. Takada, Progress and prospective of solid-state lithium batteries, Acta Mater. 61 (2013) 759–770.
- [20] A. Wang, S. Kadam, H. Li, S. Shi, Y. Qi, Review on modeling of the anode solid electrolyte interphase (SEI) for lithium-ion batteries, npj Comput. Mater. 4 (2018) 15.
- [21] X. Yu, A. Manthiram, Nitrogen goes around, Energy Environ. Sci. 11 (2018) 527–543.
- [22] L. Porz, T. Swamy, B.W. Sheldon, D. Rettenwander, T. Frömling, H.L. Thaman, S. Berendts, R. Uecker, W.C. Carter, Y.M. Chiang, Mechanism of lithium metal penetration through inorganic solid electrolytes, Adv. Energy Mater. 7 (2017), 1701003.
- [23] R. Garcia-Mendez, F. Mizuno, R. Zhang, T.S. Arthur, J. Sakamoto, Effect of processing conditions of 75Li2S-25P2S5 solid electrolyte on its DC electrochemical behavior, Electrochim. Acta 237 (2017) 144–151.

- [24] M. Nagao, A. Hayashi, M. Tatsumisago, T. Kanetsuku, T. Tsuda, S. Kuwabata, In situ SEM study of a lithium deposition and dissolution mechanism in a bulk-type solid-state cell with a Li2S–P2S5 solid electrolyte, Phys. Chem. Chem. Phys. 15 (2013) 18600–18606.
- [25] R.-Z. Qin, Y. Wang, Q.-H. Zhao, K. Yang, F. Pan, Super-dominant pathobiontic bacteria in the nasopharyngeal microbiota as causative agents of secondary bacterial infection in influenza patients, Chin. J. Struct. Chem. 39 (2020) 605–614.
- [26] J. Liu, Z. Bao, Y. Cui, E.J. Dufek, J.B. Goodenough, P. Khalifah, Q. Li, B.Y. Liaw, P. Liu, A. Manthiram, Y.S. Meng, V.R. Subramanian, M.F. Toney, V. V. Viswanathan, M.S. Whittingham, J. Xiao, W. Xu, J. Yang, X.-Q. Yang, J.-G. Zhang, Pathways for practical high-energy long-cycling lithium metal batteries, Nat. Energy 4 (2019) 180–186.
- [27] X. Fan, X. Ji, F. Han, J. Yue, J. Chen, L. Chen, T. Deng, J. Jiang, C. Wang, Fluorinated solid electrolyte interphase enables highly reversible solid-state Li metal battery, Sci. Adv. 4 (2018) eaau9245.
- [28] Q. Cheng, A. Li, N. Li, S. Li, A. Zangiabadi, T.-D. Li, W. Huang, A.C. Li, T. Jin, Q. Song, W. Xu, N. Ni, H. Zhai, M. Dontigny, K. Zaghib, X. Chuan, D. Su, K. Yan, Y. Yang, Stabilizing solid electrolyte-anode interface in Li-metal batteries by boron nitride-based nanocomposite coating, Joule 3 (2019) 1510–1522.
- [29] J. Hu, Z. Yao, K. Chen, C. Li, High-conductivity open framework fluorinated electrolyte bonded by solidified ionic liquid wires for solid-state Li metal batteries, Energy Storage Mater. 28 (2020) 37–46.
- [30] M. Lei, S. Fan, Y. Yu, J. Hu, K. Chen, Y. Gu, C. Wu, Y. Zhang, C. Li, NASICON-based solid state Li-Fe-F conversion batteries enabled by multi-interface-compatible sericin protein buffer layer, Energy Storage Mater. 47 (2022) 551–560.
- [31] H.-K. Tian, Z. Liu, Y. Ji, L.-Q. Chen, Y. Qi, Interfacial electronic properties dictate Li dendrite growth in solid electrolytes, Chem. Mater. 31 (2019) 7351–7359.
- [32] H.-K. Tian, B. Xu, Y. Qi, Nitrated T helper cell epitopes enhance the immunogenicity of HER2 vaccine and induce anti-tumor immunity, J. Power Sources 392 (2018) 79–86.
- [33] Y. Gao, D. Wang, Y.C. Li, Z. Yu, T.E. Mallouk, D. Wang, Salt-based organic-inorganic nanocomposites: towards a stable lithium metal/Li10GeP2S12 solid electrolyte interface, Angew. Chem. Int. Ed. 57 (2018) 13608–13612.
- [34] Y. Sun, J. Han, S. Myung, S. Lee, K. Amine, Significant improvement of high voltage cycling behavior AlF3-coated LiCoO2 cathode, Electrochem. Commun. 8 (2006) 821–826.
- [35] Z. Zhang, S. Chen, J. Yang, J. Wang, L. Yao, X. Yao, P. Cui, X. Xu, Interface reengineering of Li10GeP2S12 electrolyte and lithium anode for all-solid-state lithium batteries with ultralong cycle life, ACS Appl. Mater. Interfaces 10 (2018) 2556–2565.
- [36] C. Wang, Y. Gong, B. Liu, K. Fu, Y. Yao, E. Hitz, Y. Li, J. Dai, S. Xu, W. Luo, E. D. Wachsman, L. Hu, Conformal, nanoscale ZnO surface modification of garnet-based solid-state electrolyte for lithium metal anodes, Nano Lett. 17 (2017) 565–571.
- [37] B. Liu, J. Yang, H. Yang, C. Ye, Y. Mao, J. Wang, S. Shi, J. Yang, W. Zhang, Rationalizing the interphase stability of Li=doped-Li7La3Zr2O12viaautomated reaction screening and machine learning, J. Mater. Chem. A 7 (2019) 19961–19969
- [38] G. Hu, M. Zhang, L. Wu, Z. Peng, K. Du, Y. Cao, Gene expression profiles and bioinformatics analysis of human umbilical vein endothelial cells exposed to PM2.5, J. Alloy. Compd. 690 (2017) 589–597.
- [39] J. Ma, R. Quhe, Z. Zhang, C. Yang, X. Zhang, J. Li, L. Xu, J. Yang, B. Shi, S. Liu, L. Xu, X. Sun, J. Lu, Two-dimensional materials as a stabilized interphase for the solid-state electrolyte Li10GeP2S12in lithium metal batteries, J. Mater. Chem. A 9 (2021) 4810–4821
- [40] B. Liu, D. Wang, M. Avdeev, S. Shi, J. Yang, W. Zhang, High-throughput computational screening of Li-containing fluorides for battery cathode coatings, ACS Sustain. Chem. Eng. 8 (2019) 948–957.
- [41] Y. Xiao, L.J. Miara, Y. Wang, G. Ceder, Computational screening of cathode coatings for solid-state batteries, Joule 3 (2019) 1252–1275.
- [42] M. Aykol, S. Kim, V.I. Hegde, D. Snydacker, Z. Lu, S. Hao, S. Kirklin, D. Morgan, C. Wolverton, High-throughput computational design of cathode coatings for Li-ion batteries, Nat. Commun. 7 (2016) 13779.
- [43] A. Belsky, M. Hellenbrandt, V.L. Karena, P. Luksch, New developments in the inorganic crystal structure database (ICSD): accessibility in support of materials research and design, Acta Cryst. B58 (2002) 364–369.
- [44] G. Kresse, J. Furthmüller, Efficient iterative schemes for ab initio total-energy calculations using a plane-wave basis set, Phys. Rev. B 54 (1996) 11169–11186.
- [45] G. Kresse, D. Joubert, From ultrasoft pseudopotentials to the projector augmentedwave method, Phys. Rev. B 59 (1999) 1758–1775.
- [46] J.P. Perdew, K. Burke, M. Ernzerhof, Generalized gradient approximation made simple, Phys. Rev. Lett. 77 (1996) 3865–3868.
- [47] J.P. Perdew, J.A. Chevary, S.H. Vosko, K.A. Jackson, M.R. Pederson, D.J. Singh, C. Fiolhais, Atoms, molecules, solids, and surfaces: Applications of the generalized gradient approximation for exchange and correlation, Phys. Rev. B 46 (1992) 6671–6687.
- [48] H.J. Monkhorst, J.D. Pack, Special points for Brillouin-zone integrations, Phys. Rev. B 13 (1976) 5188–5192.
- [49] A. Jain, S.P. Ong, G. Hautier, W. Chen, W.D. Richards, S. Dacek, S. Cholia, D. Gunter, D. Skinner, G. Ceder, K.A. Persson, Commentary: the materials project: a materials genome approach to accelerating materials innovation, APL Mater. 1 (2013), 011002.
- [50] H. Chen, L.L. Wong, S. Adams, Acta Cryst. B75 (2019) 18-33.
- [51] S.P. Ong, W.D. Richards, A. Jain, G. Hautier, M. Kocher, S. Cholia, D. Gunter, V. L. Chevrier, K.A. Persson, G. Ceder, Python Materials Genomics (pymatgen): a

- robust, open-source python library for materials analysis, Comp. Mater. Sci. 68 (2013) 314–319.
- [52] Y. Zhu, X. He, Y. Mo, First principles study on electrochemical and chemical stability of solid electrolyte–electrode interfaces in all-solid-state Li-ion batteries, J. Mater. Chem. A 4 (2016) 3253–3266.
- [53] Y. Zhu, X. He, Y. Mo, Origin of outstanding stability in the lithium solid electrolyte materials: insights from thermodynamic analyses based on first-principles calculations, ACS Appl. Mater. Interfaces 7 (2015) 23685–23693.
- [54] W.D. Richards, L.J. Miara, Y. Wang, J.C. Kim, G. Ceder, Interface stability in solidstate batteries, Chem. Mater. 28 (2015) 266–273.
- [55] C. Ma, Y. Cheng, K. Yin, J. Luo, A. Sharafi, J. Sakamoto, J. Li, K.L. More, N. J. Dudney, M. Chi, Interfacial stability of Li metal-solid electrolyte elucidated via in situ electron microscopy, Nano Lett. 16 (2016) 7030–7036.
- [56] F. Han, Y. Zhu, X. He, Y. Mo, C. Wang, Electrochemical stability of Li10GeP2S12 and Li7La3Zr2O12 solid electrolytes, Adv. Energy Mater. 6 (2016), 1501590.
- [57] M.M. Besli, C. Usubelli, M. Metzger, V. Pande, K. Harry, D. Nordlund, S. Sainio, J. Christensen, M.M. Doeff, S. Kuppan, Effect of liquid electrolyte soaking on the interfacial resistance of Li7La3Zr2O12 for all-solid-state lithium batteries, ACS Appl. Mater. Interfaces 12 (2020) 20605–20612.
- [58] L. Cheng, E.J. Crumlin, W. Chen, R. Qiao, H. Hou, S. Franz Lux, V. Zorba, R. Russo, R. Kostecki, Z. Liu, K. Persson, W. Yang, J. Cabana, T. Richardson, G. Chen, M. Doeff, The origin of high electrolyte-electrode interfacial resistances in lithium cells containing garnet type solid electrolytes, Phys. Chem. Chem. Phys. 16 (2014) 18294–18300.
- [59] R. Xu, F. Han, X. Ji, X. Fan, J. Tu, C. Wang, Interface engineering of sulfide electrolytes for all-solid-state lithium batteries, Nano Energy 53 (2018) 958–966.
- [60] F. Han, J. Yue, X. Zhu, C. Wang, Suppressing Li dendrite formation in Li2S-P2S5 solid electrolyte by LiI Incorporation, Adv. Energy Mater. 8 (2018), 1703644.
- [61] S. Ohta, S. Komagata, J. Seki, T. Saeki, S. Morishita, T. Asaoka, All-solid-state lithium ion battery using garnet-type oxide and Li3BO3 solid electrolytes fabricated by screen-printing, J. Power Sources 238 (2013) 53–56.
- [62] George V. Alexander, N.C. Rosero-Navarro, A. Miura, K. Tadanaga, R. Murugan, Electrochemical performance of a garnet solid electrolyte based lithium metal battery with interface modification, J. Mater. Chem. A 6 (2018) 21018–21028.



Simo Li received his M. S. degree in Prof. Feng Pan's group at School of Advanced Materials, Peking University, Shenzhen Graduate School, China. He received his B.S. degree in Chemistry from Wuhan University in 2019. His current research mainly focuses on first-principles study of the electrochemical and thermodynamics properties of solid-state electrolytes in lithium-ion batteries.



Zhefeng Chen received his B.E. degree in 2018 from School of Physics, Peking University, China. He is now a Ph.D. student in the School of Advanced Materials, Peking University, Shenzhen Graduate School, China. His research interest includes first-principles design of energy storage materials.



Wentao Zhang received his B.E. degree in 2019 from School of Materials Science and Engineering, Central South University, China. He is now a Ph.D. student in the School of Advanced Materials, Peking University, Shenzhen Graduate School, China. His research interest includes computational design of energy storage materials via combined first-principles calculations and machine learning techniques.

S. Li et al. Nano Energy 102 (2022) 107640



Shunning Li received his B.E. degree in 2013 and Ph.D. degree in 2018 from School of Materials Science and Engineering, Tsinghua University, China. Currently, he is an associate research fellow at the School of Advanced Materials, Peking University, Shenzhen Graduate School, China. His research mainly focuses on first-principles simulations of electrochemical reactions, and machine-learning-assisted materials design for energy storage and conversion.



Feng Pan, Chair-Professor, VP of Peking University, Shenzhen Graduate School, Founding Dean of School of Advanced Materials, Director of National Center of Electric Vehicle Power Battery and Materials for International Research, received his B.S. degree from Dept. Chemistry, Peking University in 1985 and Ph.D. from Dept. of P & A Chemistry, University of Strathclyde, UK with "Patrick D. Ritchie Prize" for the best Ph. D. in 1994. Prof. Pan has been engaged in fundamental research of structure chemistry, exploring "Material Gene" for Li-ion batteries and developing novel energy conversion/storage materials & devices. He also received the 2018 ECS Battery Division Technology Award (US), and 2021 China Electro-

chemistry Contribution Award